

Using Ocean Gliders to Understand the Physical Oceanography of Fitz Hugh Sound

by

Martin Williamson

A Thesis Submitted in Partial Fulfillment of the
Requirements of the

HONOURS PROGRAM

in the School of Earth and Ocean Sciences

Supervisor: Dr. Jody Klymak

© Martin Williamson, 2026
University of Victoria

All rights reserved. This thesis may not be reproduced in whole or in part,
by photocopy or other means, without the permission of the author.

We acknowledge and respect the Lək'wəŋən (Songhees and X^wsepsəm/Esquimalt) Peoples
on whose territory the university stands, and the Lək'wəŋən and W̱SÁNEĆ Peoples whose
historical relationships with the land continue to this day.



**University
of Victoria**

University of Victoria

DEPARTMENT OF EARTH & OCEAN SCIENCES

**Using Ocean Gliders to Understand the Physical
Oceanography of Fitz Hugh Sound**

Honours Thesis

in partial fulfillment of the requirements of the Earth & Ocean Sciences Honours Program

March 2026

by

Martin Williamson

Supervisor: Dr. Jody Klymak

Contents

1	Introduction	6
2	Sites and Methods	10
2.1	Study Area	10
2.2	Ocean Gliders and Data Processing	10
3	Results	12
3.1	Deep Water Renewal	13
3.2	Vertical Mixing	16
3.3	Winter Renewal	19
3.4	Oxygen variability	21
4	Discussion	25
4.1	Estimating a critical flow speed at the sill	25
4.2	Mixing and oxygen modification during renewal	30
4.3	Vertical diffusion rate	32
5	Conclusions	36
6	Supplementary remarks	38
7	Acknowledgements	39

List of Figures

1	Map of the study region with bathymetric contours at 25m intervals. The dashed magenta line represents a typical glider track starting in Fitz Hugh Sound. Red markers represent Hakai CTD survey stations, green markers represent distance along a transect in a curvilinear coordinate system, and the blue marker represents the Hakai Passage sill, which is defined as the 0 km point along the glider transects.	9
2	A C-PROOF ocean glider, dfo-marvin1003, during a deployment out of the Bamfield Marine Science Centre (BMSC) in Barkley Sound, off the west coast of Vancouver Island, B.C., on July 9th, 2025. A significant Coccolithopore bloom is attributed to the unusual ocean colour.	12
3	Potential temperature θ ($^{\circ}\text{C}$) sections along the Calvert Line from March 2024 to March 2025. Panels are arranged in chronological order from left to right, top to bottom. Contours show potential density, σ_{θ} (kg m^{-3}): black isopycnals are spaced at $0.5 \sigma_{\theta}$, while the coloured lines highlight isopycnals from $25.5 \sigma_{\theta}$ to $26.5 \sigma_{\theta}$ at intervals of $0.1\sigma_{\theta}$	14
4	Salinity (PSU) sections along the Calvert Line from March 2024 to March 2025. Panels are arranged in chronological order from left to right, top to bottom. Contours show potential density, σ_{θ} (kg m^{-3}): black isopycnals are spaced at $0.5 \sigma_{\theta}$, while the coloured lines highlight isopycnals from $25.5 \sigma_{\theta}$ to $26.5 \sigma_{\theta}$ at intervals of $0.1\sigma_{\theta}$	17
5	Profiles of glider data and hakai data in the FHS deep basin during the fall and winter of 2024 - 2025.	20

6	Temperature - Salinity diagram of glider data in FHS in deep basin (21.1 km along the transect, represented by the dots) and the shelf (-30 km along, represented by the crosses). Contoured is potential density, σ_θ (kg m^{-3}): black isopycnals are spaced at $0.5 \sigma_\theta$, while the coloured lines represent isopycnals from $25.5 \sigma_\theta$ to $26.5 \sigma_\theta$ at intervals of 0.1.	21
7	Oxygen ($\mu\text{mol L}^{-1}$) time series from March 2024 until August 2025. Contoured is potential density, σ_θ (kg m^{-3}): black isopycnals are spaced at $0.5 \sigma_\theta$, while the coloured lines represent isopycnals from $25.5 \sigma_\theta$ to $26.5 \sigma_\theta$ at intervals of 0.1.	22
8	Oxygen [$\mu\text{mol L}^{-1}$]sections along the Calvert Line from March 2024 to May 2025. Panels are arranged in chronological order from left to right, top to bottom. Contours show potential density, σ_θ (kg m^{-3}): black isopycnals are spaced at $0.5 \sigma_\theta$, while the coloured lines highlight isopycnals from $25.5 \sigma_\theta$ to $26.5 \sigma_\theta$ at intervals of $0.1\sigma_\theta$. Red contours near the ocean floor indicate hypoxic conditions or concentrations below $61 \mu\text{mol L}^{-1}$	24
9	Potential temperature ($^\circ\text{C}$) time series from March 2024 until August 2025 at 4 locations. The dashed horizontal black line represents the HP sill depth (130 m). In order from top the bottom the panels are: the QCS shelf (-30 km), the HP sill (0 km), (near) the southern FHS sill (QCS07), and the FHS deep basin (21.1 km). Contoured is potential density, σ_θ (kg m^{-3}): black isopycnals are spaced at $0.5 \sigma_\theta$, while the coloured lines represent isopycnals from $25.5 \sigma_\theta$ to $26.5 \sigma_\theta$ at intervals of 0.1.	26

10	Salinity (PSU) time series from March 2024 until August 2025 at 4 locations. The dashed horizontal black line represents the HP sill depth (130 m). In order from top the bottom the panels are: the QCS shelf (−30 km), the HP sill (0 km), (near) the southern FHS sill (QCS07), and the FHS deep basin (21.1 km). Contoured is potential density, σ_θ (kg m^{-3}): black isopycnals are spaced at $0.5 \sigma_\theta$, while the coloured lines represent isopycnals from $25.5 \sigma_\theta$ to $26.5 \sigma_\theta$ at intervals of 0.1.	27
11	Histogram of all glider data from 2024 and 2025 for potential temperature θ ($^\circ\text{C}$) and salinity (psu) on the left panel, and potential density σ_θ (kg m^{-3}) plotted against oxygen $\mu\text{mol L}^{-1}$ on the right. The hypoxic limit of $61 \mu\text{mol L}^{-1}$ is plotted as a dashed red line. Data is binned to 0.01 ($^\circ\text{C}$), 0.01 psu, 0.01(kg m^{-3}), and $1 \mu\text{mol L}^{-1}$. Density anomaly 26.5 kg m^{-3} is plotted as a dashed white line on the right panel.	31
12	Potential temperature θ ($^\circ\text{C}$) sections along the Calvert Line from March 2024 to January 2026. Panels are arranged in chronological order from left to right, top to bottom. Contours show potential density, σ_θ (kg m^{-3}): black isopycnals are spaced at $0.5 \sigma_\theta$, while the coloured lines highlight isopycnals from $25.5 \sigma_\theta$ to $26.5 \sigma_\theta$ at intervals of $0.1\sigma_\theta$	43
13	Salinity (PSU) sections along the Calvert Line from March 2024 to January 2026. Panels are arranged in chronological order from left to right, top to bottom. Contours show potential density, σ_θ (kg m^{-3}): black isopycnals are spaced at $0.5 \sigma_\theta$, while the coloured lines highlight isopycnals from $25.5 \sigma_\theta$ to $26.5 \sigma_\theta$ at intervals of $0.1\sigma_\theta$	44

Abstract

Autonomous glider transects from Queen Charlotte Sound (QCS) into Fitz Hugh Sound (FHS) provide high resolution cross-sections of temperature, salinity, density, and oxygen that reveal the dynamics of deep-water renewal and vertical mixing in a deep-silled fjord on the central coast of British Columbia. Glider transects collected between March 2024 and August 2025 were analyzed alongside Hakai CTD surveys to document the timing, structure, and modification of renewal flows. Renewal primarily occurs as a summertime process, with dense QCS shelf water flowing over the Hakai Passage (HP) sill and flushing the FHS deep basin, with an upper layer of FHS water leaving through HP as a return flow. Renewal appears to occur over the HP sill as opposed to the wider southern sill. A temperature - salinity parameter space comparison suggests that weaker winter renewal can also occur, bringing higher oxygen water into the deep basin. Simple two-layer hydraulic control estimates give upper bound flow velocities of $0.6\text{-}0.7\text{ m s}^{-1}$ and volumetric fluxes of $3.6\text{-}4.2 \times 10^4\text{ m}^3\text{ s}^{-1}$, implying a characteristic deep basin flushing timescale of roughly 15-19 days during renewal conditions. Vertical diffusivity estimates based on conservative tracers yield values on the order of $10^{-3}\text{ m}^2\text{ s}^{-1}$, consistent with previous studies in similar British Columbia fjords and waterways. Although source waters on the shelf occasionally reached hypoxic concentrations during the study period, mixing over the sill and along the renewal flow path increased oxygen levels, preventing hypoxia in the FHS deep basin. These results highlight the role of sill mixing in buffering deep fjord basins from hypoxic shelf source water, but also suggest that future declines in oxygen on the QCS shelf could overcome this protection if water of lesser density becomes hypoxic.

1 Introduction

Fitz Hugh Sound (FHS), off the central coast of British Columbia and to the east of Queen Charlotte Sound (QCS), is a deep fjord-like waterway that is connected to QCS by two sills: a relatively narrow 130 m deep sill in Hakai Passage (HP) to the north of Calvert Island, and a broader 120 m deep sill to the south between Calvert Island and the mainland (Figure 1). Its deep inner basin plunges to 420 m, a depth much greater than the adjacent QCS shelf. With a mean mid-channel depth of 330 m, FHS is typical of many glacially carved inlets on the B.C. coast: it maintains a fresh surface layer and estuarine circulation, with deep water (defined as water below the sill depth) experiencing fluctuations in density on an annual time scale (Evans, 2024). The estuarine circulation is driven by freshwater river input at the heads of Dean channel and Burke channel, whose mouths connect to FHS in the north, with runoff peaking with the freshet between June and August (Dodimead and Herlinveaux, 1968; Pickard, 1961).

Deep water renewal in a fjord occurs when water outside the fjord at the sill is denser than the resident deep water. The resulting pressure gradient drives dense water over the sill, where it propagates as a gravity current descending into the deep basin, replacing and flushing resident deep water upwards and out (Farmer and Freeland, 1983). In an idealized case without mixing, the renewed deep water would retain the same physical properties as the sill water. In reality, gravity currents experience mixing through a variety of processes, such as hydraulic jumps and turbulent mixing. Mixing entrains surrounding fluid, modifying oxygen concentrations and reducing the density of the renewal water as it enters the deep basin (Farmer and Freeland, 1983). Consequently, the duration and frequency of renewals in fjords is highly variable. Some fjords in B.C. with deep sill depths (>100 m), such as that of Trevor Channel and Alberni Inlet (100 m sill) may experience continuous renewal events over a period of weeks to months, dependent on the availability of dense water at the sill and the amount of entrainment that occurs. Under this regime, deep basin water properties usually adjust rapidly to those of the adjacent shelf (Pawlowicz, 2017). In the case of fjords

with shallower sills, such as Saanich Inlet with a 70 m deep sill, significant tidal mixing can reduce the density of renewal water as it passes over the sill. Renewal events are thus highly episodic and dependent on low tidal current speeds, sometimes with multiple discrete renewal events needed in order to supply enough dense water to displace the deepest resident water in the basin (Manning et al., 2010; Soetaert et al., 2022).

Since 2019, the C-PROOF (Canadian Pacific Robotic Ocean Observing Facility) (Klymak and Ross, 2025) glider program has been developing a time series of high resolution transects by sending autonomous ocean gliders on monitoring missions. One of these monitoring lines is the Calvert Line (dashed magenta line in Figure 1), which starts in FHS, crosses the QCS shelf and travels out into the deep ocean to station P16 (Klymak and Ross, 2025). Previous studies have shown that QCS summertime shelf bottom water has experienced a long term trend of declining O_2 concentrations at approximately 5-10 $\mu\text{mol kg}^{-1}$ per decade, and despite recent emergence of widespread summertime hypoxia (2022, 2023) (defined as $[O_2] > 61 \mu\text{mol kg}^{-1}$) being attributed to interannual and decadal scale variability, projections suggest that summer hypoxia will be the norm by 2050 (Stevens et al., 2025a). Another study found that while persistent summer upwelling is the most likely mechanism to deliver low oxygen water to FHS, the low oxygen values observed on QCS shelf bottom water (the most likely source for FHS renewal water) did not appear to extend landward from FHS into Burke and Dean Channel, suggesting there may be modification of renewal water through mixing over geographical features (Evans, 2024).

This study analyzes high-resolution, two-dimensional glider transects starting from Calvert Island and Fitz Hugh Sound between March 2024 and January 2026, along with supplementary CTD data collected by the Hakai Institute, to understand and quantify the physical processes that modify deep water in Fitz Hugh Sound. This work provides a clearer understanding of deep water dynamics in Fitz Hugh Sound by documenting and quantifying the timing, structure, and modification of renewal flows over the sill as well as vertical mixing in the deep basin during periods of isolation from the shelf. This work provides a critical under-

standing of the physical oceanography of Fitz Hugh Sound within the context of emerging hypoxia off the BC coast.

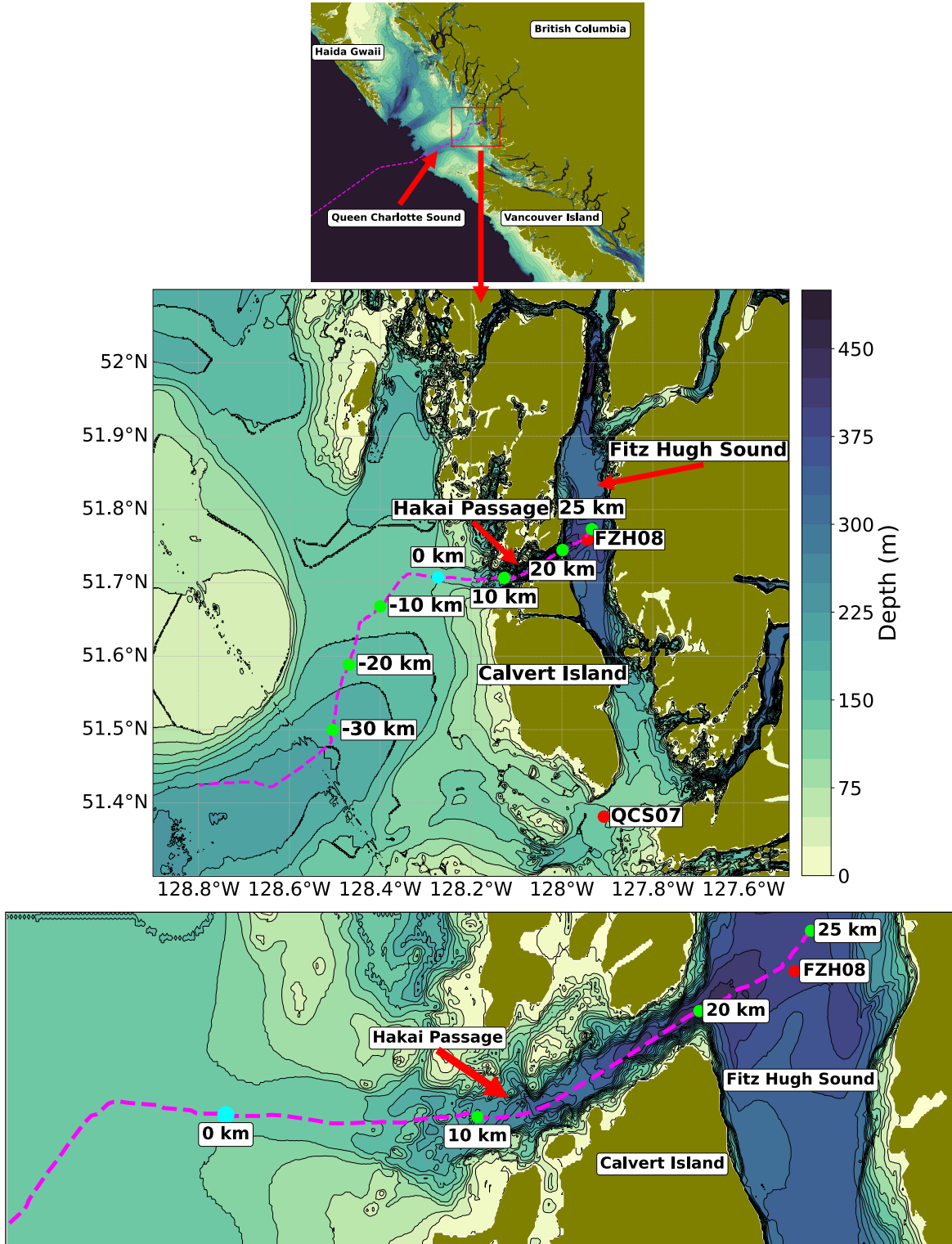


Figure 1: Map of the study region with bathymetric contours at 25m intervals. The dashed magenta line represents a typical glider track starting in Fitz Hugh Sound. Red markers represent Hakai CTD survey stations, green markers represent distance along a transect in a curvilinear coordinate system, and the blue marker represents the Hakai Passage sill, which is defined as the 0 km point along the glider transects.

2 Sites and Methods

2.1 Study Area

This study focuses on roughly 55 km of glider data near Calvert Island, BC, over a series of transects from March 2024 to January 2026. Glider missions typically begin in the deep basin of Fitz Hugh Sound (FHS). From there, gliders travel southwest through Hakai Passage (HP), and then turn west as they travel up and over a 130 m deep sill, and out onto the Queen Charlotte Sound (QCS) shelf (Figure 1). Once having crossed the shelf through Goose Trough, gliders continue out into the open ocean until they reach station P16 before returning along the same transect. Missions typically take between 7-8 weeks. This study uses an “along” transect coordinate system (km), with the sill in Hakai Passage (the “HP sill”) being defined as 0 km. Offshore of the HP sill towards QCS is defined as the negative direction (west) while east into HP and FHS from the sill is positive. The sill is approximately 2 km wide. Between the HP sill and FHS, the bathymetry of HP is that of a deep sloping trough that plunges down to approximately 420 m as it opens into the deep FHS basin. The deep FHS basin shoals slightly as it extends to the north towards the Burke and Dean channels, but shoals more significantly towards the south with a 120 m sill between Calvert Island and the mainland.

2.2 Ocean Gliders and Data Processing

An ocean glider, pictured in Figure 2, has a buoyancy engine that allows it to move vertically through the water column. Using hydrodynamic wings, it can turn some of its vertical motion into forward thrust (Klymak and Ross, 2025). C-PROOF gliders are equipped with a RBR Legato CTD, an RBR Duet3 Oxygen sensor, a Wetlabs FLBBCDSLFC fluorometer and backscatter sensor, and a pressure sensor. As it travels, the glider collects measurements during both up and down profiles to map out a cross sectional transect of the ocean. Data is initially processed as per the C-PROOF processing standard, and data used in this report is

from the ‘_grid_CTDadjusted.nc’ files from the Calvert Line during 2024 and 2025 ([Klymak and Ross, 2025](#)).

Further processing includes projecting the gliders latitude and longitude from each vertical profile onto an “along” coordinate system (x-direction) representing the typical glider transect, interpolation to a 50 m grid, and a larger grid interpolation algorithm to fill in the FHS deep basin. The deep basin interpolation algorithm, which takes all existing deep basin profiles and interpolates between them horizontally, was applied to the dataset used for this study since there tends to be less spatial coverage of deep profiles in FHS as compared to other parts of the transect due to glider recovery logistics. Additional data from Hakai CTD surveys in the deep basin are used to help fill temporal gaps, and are used for a vertical diffusivity estimate comparison. Data from the Hakai Institute was taken from the Hakai ERDDAP server using the scientific CTD survey dataset for stations FZH08 and QCS07.



Figure 2: A C-PROOF ocean glider, dfo-marvin1003, during a deployment out of the Bamfield Marine Science Centre (BMSC) in Barkley Sound, off the west coast of Vancouver Island, B.C., on July 9th, 2025. A significant Coccolithopore bloom is attributed to the unusual ocean colour.

3 Results

High resolution glider transects reveal that deep water renewal and vertical mixing are the dominant and coupled processes modifying deep water and associated oxygen conditions in Fitz Hugh Sound (FHS). We will later decouple these processes quantitatively, though much can be understood from a qualitative analysis of glider transects from March 2024 to March 2025 (Figure 3). Eight transects are presented here to demonstrate the physical changes throughout the period, while a full time series of glider sections can be found in the appendix.

3.1 Deep Water Renewal

Deep water renewal typically occurs in the summer months when dense water on the shelf and at the Hakai Passage (HP) sill is denser than resident deep water in FHS, though we will show later that winter renewal can also occur. To understand renewal in FHS, we study temperature, salinity, and density conditions along the glider transects before, during, and after the renewal (Figure 3 and 4).

In March 2024, near the sill in Queen Charlotte Sound (QCS), the water column is well mixed down to the ocean floor (Figure 3). On both sides of the sill, surface waters are generally cooler and fresher than intermediate waters, with the shelf being warmer than FHS. The coldest and freshest surface water is in HP and FHS. The deep water in FHS has density anomaly $\sigma_\theta = 25.6 \text{ kg m}^{-3}$ (white), and the mixed layer is shallower than on the shelf, extending from the surface to between 50 and 100 m depth. The densest water at the sill is the $25.5 \sigma_\theta$ isopycnal (black). In the April transect, it is evident that a renewal has begun, as a cold, dense water mass has appeared at the bottom of QCS, and a sloping layer of dense water is observed along the bottom of Hakai Passage, tilted downwards towards FHS. Isopycnals have generally lifted in FHS, and the densest water at the sill is the $26.4 \sigma_\theta$ isopycnal (cyan).

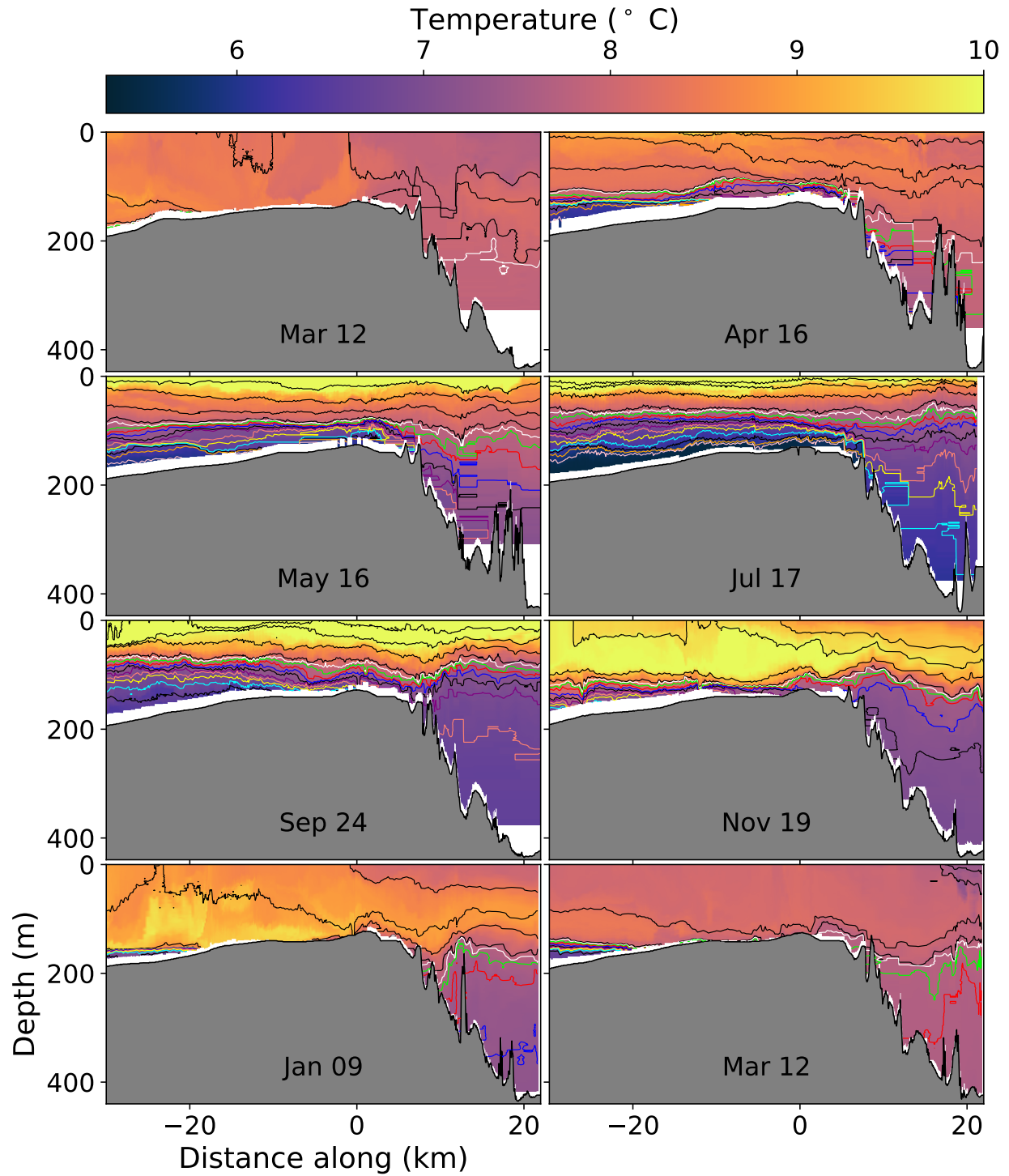


Figure 3: Potential temperature θ ($^{\circ}\text{C}$) sections along the Calvert Line from March 2024 to March 2025. Panels are arranged in chronological order from left to right, top to bottom. Contours show potential density, σ_{θ} (kg m^{-3}): black isopycnals are spaced at $0.5 \sigma_{\theta}$, while the coloured lines highlight isopycnals from $25.5 \sigma_{\theta}$ to $26.5 \sigma_{\theta}$ at intervals of $0.1 \sigma_{\theta}$.

Continuing with the April transect observations, isopycnals over the sill exhibit a downward tilt over the sill in the eastward direction, indicating a flow of renewal water is descending from QCS into HP as a gravity current. The bottom water in QCS is generally much colder and denser than deep water in HP and FHS. The 26.0 σ_θ isopycnal has appeared in the trough of HP near the 10 km mark, an increase of 0.5 σ_θ from March, confirming that renewal and flushing of older resident water is occurring.

In May, renewal continues to occur, with cold and dense water continuing to flow into HP, replacing existing deep water and flushing it upwards. Both QCS bottom water and FHS basin water is colder and denser than during the previous transect. The 25.8 σ_θ isopycnal (red) fills the deep basin, and the 25.9 σ_θ isopycnal (blue) is present at the very bottom of Hakai Passage. Isopycnal tilts over the sill suggest a gravity current is pouring down the HP trough, similar to what was observed in April, though with denser water during the May transect. Interestingly, above the inflowing layer at the HP sill, isopycnals between 24 and 25.5 σ_θ are tilted in the opposite direction as compared to the layers below, indicating a return flow. Near the surface, a typical summertime stratification pattern is generally observed, with the surface having warmed significantly, and with more stratification than during the winter when the shelf had a deep mixed layer. We note the colour bar is set to a max of 10 °C to highlight deep water temperature changes, and therefore the colour scale becomes saturated at the surface during the summer months.

In July, bottom water both in QCS and FHS is colder and denser than in May, indicating that further upwelling of cold dense water onto the shelf and subsequent further renewal of FHS deep water has occurred. The deep water in FHS has cooled, with water of 26.4 σ_θ (cyan) occupying the deepest parts of the basin. There exists water denser than the 26.5 σ_θ isopycnal over the sill, and a sharp isopycnal tilt into HP, indicating that the inflowing gravity current renewing the deep basin is ongoing.

In September, the temperature of both QCS and FHS bottom water has increased and the densest water in FHS is lighter than the July transect, suggesting that the renewal has

stopped, the basin has become somewhat isolated from the shelf, and mixing has occurred, acting to reduce the density of the deep basin. While water at the sill remains denser than deep water in FHS, similar to the spring and summer transects, there is no gravity current of dense water in Hakai Passage. These observations suggest deep water in FHS can become isolated from shelf bottom water when the upwelling of dense water to the HP sill has relaxed. We have not resolved smaller scale fluctuations such as tidal effects, which may play a role in moving water over the sill when renewal is not dominating the general circulation, and thus remains a limitation to these interpretations at this time.

3.2 Vertical Mixing

During the winter months when renewal is not occurring, vertical mixing is the dominant process that acts to remove cold, saline, dense water out of the deep basin, mixing in oxygen, heat, and fresher water from above. Between each transect from September to January, the temperature of the deep basin increases, salinity decreases, and thus density decreases (Figure 3). Under the assumption that renewal is not occurring during this time period as suggested by the section plots (Figure 3 and 4), the basin should be isolated from the shelf. Any subsequent changes in temperature, salinity, and density then indicate that vertical mixing smooths gradients between the deep basin and water above. We will later show that winter renewal can occur, and thus the deep basin isn't always isolated from shelf conditions during the winter. Later in the discussion we use observations from a period of deep basin isolation to quantify the rate K_z of vertical mixing.

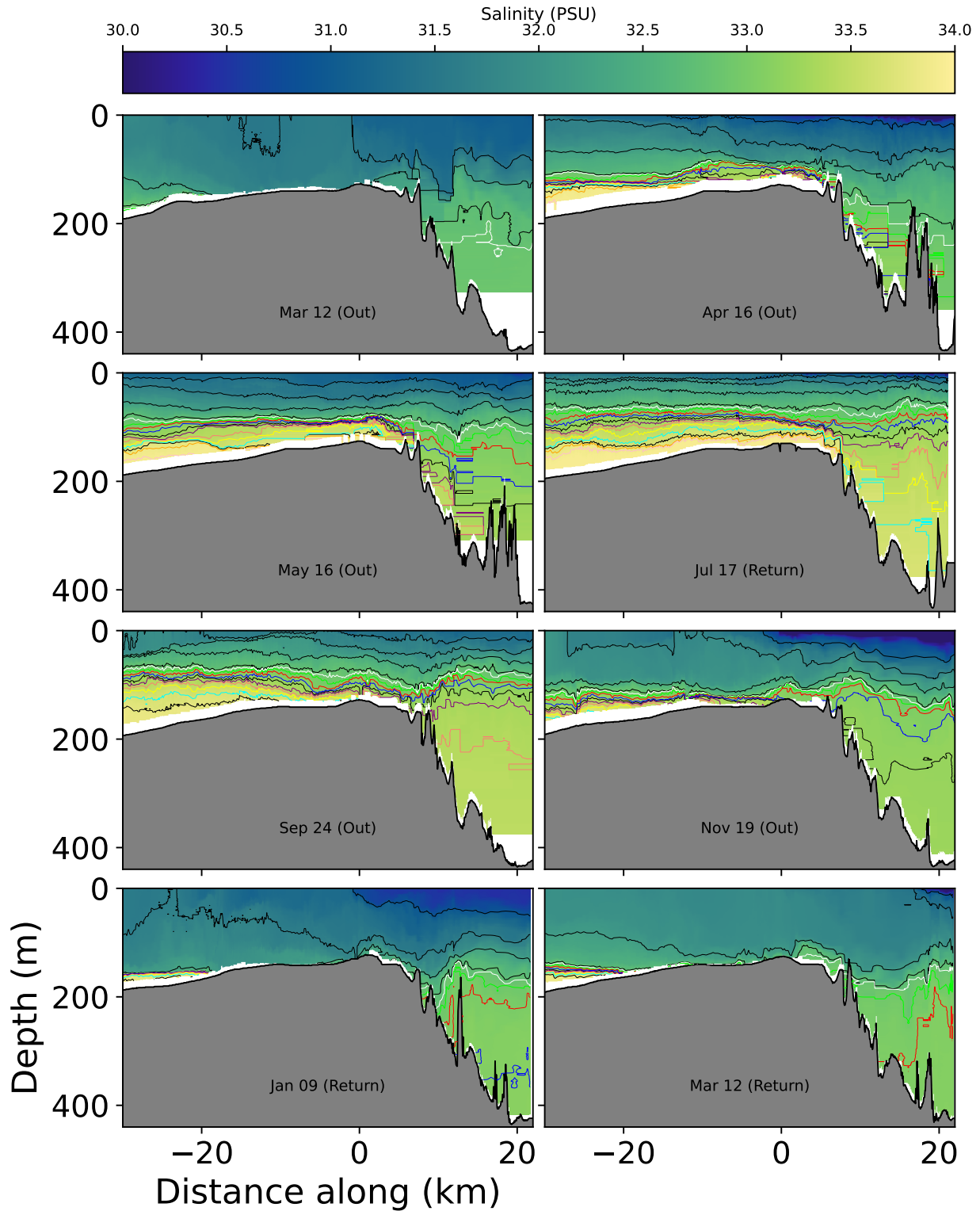


Figure 4: Salinity (PSU) sections along the Calvert Line from March 2024 to March 2025. Panels are arranged in chronological order from left to right, top to bottom. Contours show potential density, σ_θ (kg m^{-3}): black isopycnals are spaced at $0.5 \sigma_\theta$, while the coloured lines highlight isopycnals from $25.5 \sigma_\theta$ to $26.5 \sigma_\theta$ at intervals of $0.1 \sigma_\theta$.

The November transect shows that summer surface heat is being mixed downwards, the surface is cooling, and that basin density has decreased, with the 26.0 σ_θ isopycnal filling the deep basin (Figure 3 and 4). Generally, FHS is less mixed than the shelf, and a layer of cooler and fresher surface water has appeared overtop warmer water in FHS and extending out just past the HP sill, as seen in Figures 3 and 4. We suggest the surface waters in FHS and HP might be less mixed than the shelf on this transect due to the relative freshness of the surface water. Since density increases with salinity and decreases with temperature, fresher water in FHS could cool more than similar temperature water of higher salinity on the shelf would before it becomes negatively buoyant and sinks. The result of this would be less convective overturning in FHS than on the QCS shelf, which may explain the observed stratification differences between the two regions.

In January, a deep mixed layer has formed down to the ocean floor, to as deep as about 160 m in QCS. Along deeper parts of the QCS shelf, we find a strong and suppressed thermocline and pycnocline (at -30 km along in Figure 3 and 4). Along with the deep mixed layer, this may suggest that dense water is being actively suppressed by downwelling during this period. Near the sill, the entire water column is well mixed. In FHS, there is a unique layer of cooler and fresher water at the surface that is not seen out into QCS. This indicates that there is a typical estuarine circulation. We also note cooler surface waters in FHS, which could occur if there was cooler air near the coast, and or if fresher surface water (due to coastal runoff) results in less convective overturning compared with the shelf, allowing surface water to cool to a greater extent before losing its relative buoyancy. In January the deep basin has again warmed, the salinity has again decreased, and the density of the deep water has again decreased, with the densest water being the 25.9 σ_θ isopycnal (blue). This suggests vertical mixing has continued to be the dominant process from September 2024 to January 2025.

3.3 Winter Renewal

Although vertical mixing dominates much of the winter period, observations between January and March 2025 indicate that winter renewal can occur. Profiles of the basin demonstrate that while temperature increases and density decreases slightly between January and March, salinity doesn't change, and oxygen increases significantly, suggesting renewal occurred. A temperature - salinity (TS) diagram reveals deep basin TS properties match those of the shelf, confirming that renewal occurred sometime between glider transects.

In the FHS basin, along channel differences at a given depth (Hakai CTD data at FZH08 vs glider data at 21.1 km along) are generally much smaller than changes over time (Figure 5). The thermocline, halocline, pycnocline, and oxycline all occur generally above sill depth. Below 130 - 150 m, the basin is weakly stratified, with minimal changes in properties with depth in the deepest parts of the basin. From September to November, temperature increases, salinity decreases, density decreases, indicating vertical mixing is the dominant process, smoothing gradients of conservative tracers between the deep basin and water above. From September to January, oxygen changes are minimal, which may suggest vertical mixing is replenishing oxygen at a similar rate as the respiration of organic matter.

From January to March, temperature increases, salinity doesn't change significantly, density decreases slightly, and oxygen increases significantly. Changes in oxygen are due to both vertical mixing and background respiration rates, and so factors explaining the sudden change in oxygen concentrations could be that the rate of vertical mixing K_z suddenly became much stronger, that background respiration suddenly became significantly smaller, or that deep water renewal occurred, bringing higher oxygen water to the basin. All of these processes are coupled, with the resultant oxygen signal being a superposition of the relative effect each process has on modifying water properties. Thus, to distinguish between these possibilities, we examine the profiles in TS parameter space.

Observations in TS space reveal that a winter renewal occurred between January and March, since deep basin TS properties match those of the shelf almost exactly (Figure 6). In

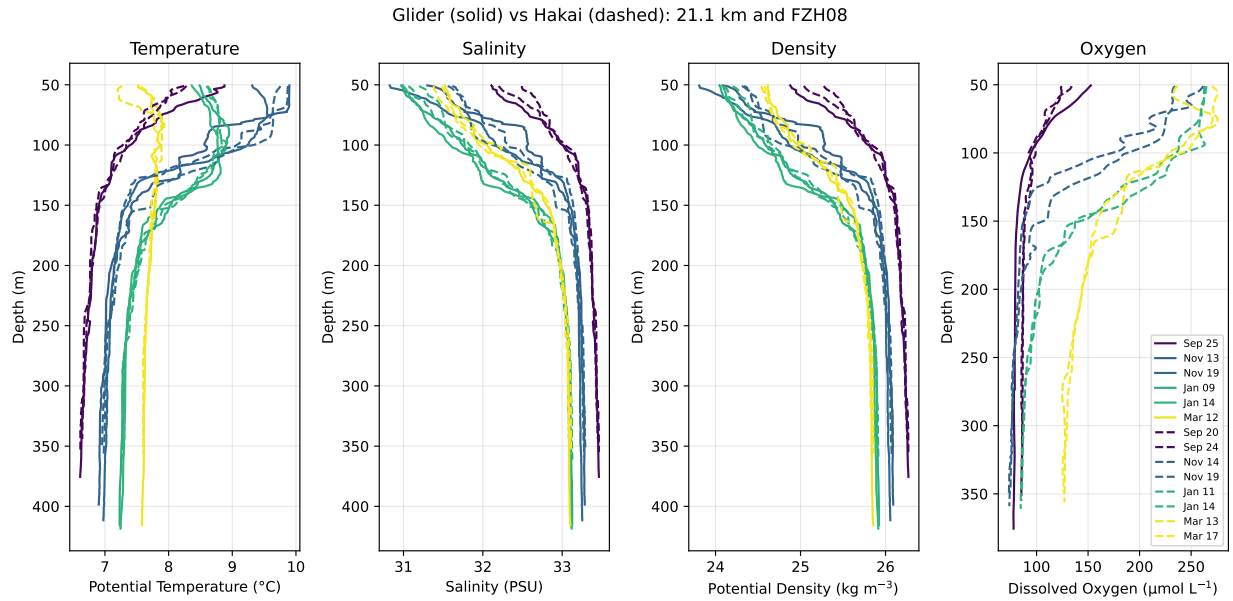


Figure 5: Profiles of glider data and hakai data in the FHS deep basin during the fall and winter of 2024 - 2025.

September, November, and January, TS properties between the shelf and the deep basin are different, indicating different water masses at each location, and that the basin is isolated during those months, supporting the conclusion that vertical mixing is dominant during that time period. In March, the densest basin water matches shelf properties exactly, indicating that a renewal occurred between the January and March transects. We also note that a number of data points for TS properties on the shelf match up well with winter deep basin water properties from months previous, which may suggest that some of the basin water ended up on the shelf after being flushed, though further comparison of TS properties at different locations may be needed to better support this.

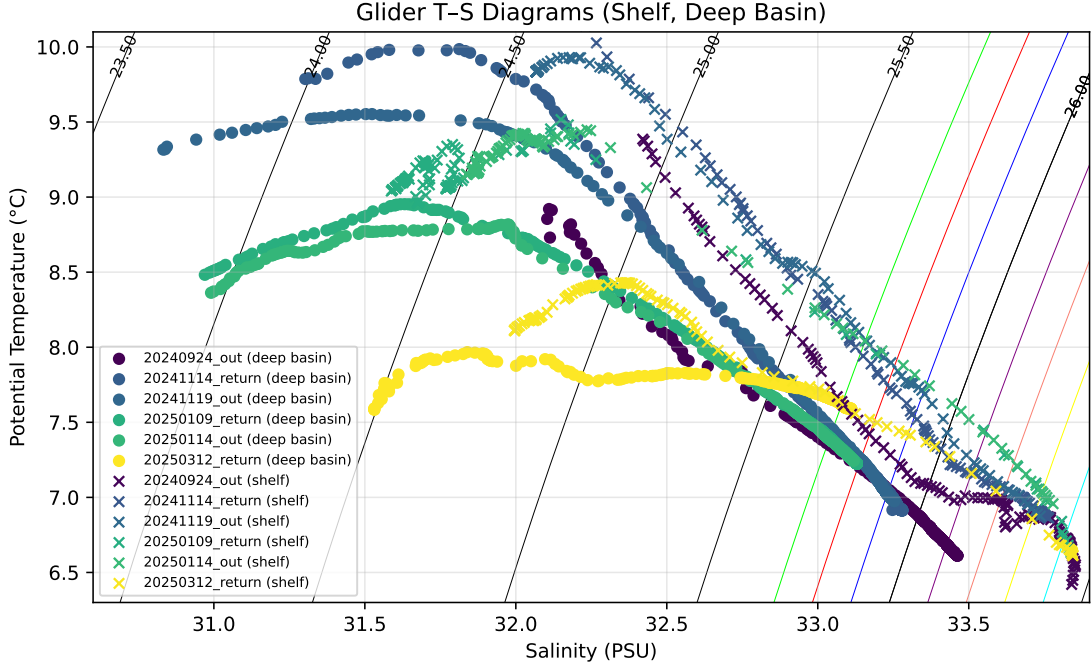


Figure 6: Temperature - Salinity diagram of glider data in FHS in deep basin (21.1 km along the transect, represented by the dots) and the shelf (-30 km along, represented by the crosses). Contoured is potential density, σ_θ (kg m^{-3}): black isopycnals are spaced at $0.5 \sigma_\theta$, while the coloured lines represent isopycnals from $25.5 \sigma_\theta$ to $26.5 \sigma_\theta$ at intervals of 0.1 .

3.4 Oxygen variability

Oxygen in the deep basin exhibits a strong seasonal cycle, with lower concentrations during summer when renewal is bringing low oxygen water to the deep basin, and higher concentrations during winter (Figure 7) when vertical mixing and deep water renewal brings higher O_2 water. This means that deep water renewal can bring both high and low oxygen water to Fitz Hugh Sound depending on source conditions, while mixing along the flow path, background vertical mixing, and respiration are all processes whose effect on the observed oxygen signal are coupled.

Considering oxygen concentrations for a given vertical profile, O_2 is usually highest at the surface and decreases with depth (Figure 7 and 8). At the surface, water can freely exchange O_2 with the atmosphere. From the surface σ_θ down through the euphotic zone, oxygen is added through photosynthesis and mixing with the surface, and it is removed by the respiration

of organic matter. The observed O_2 signal is therefore a superposition of the sources and sinks. At depth, below the euphotic zone, and far away from the surface, there is no primary production occurring, and thus water has less O_2 , since the dominant process modifying O_2 is the respiration of organic matter. Thus, for deeper water to experience an increase in O_2 , rates of lateral advection of higher O_2 water or vertical mixing bringing down O_2 from above must be greater than background respiration rates. While these processes are all superimposed onto the observed oxygen signal (Figure 7), we can delineate which processes dominate at which times of year.

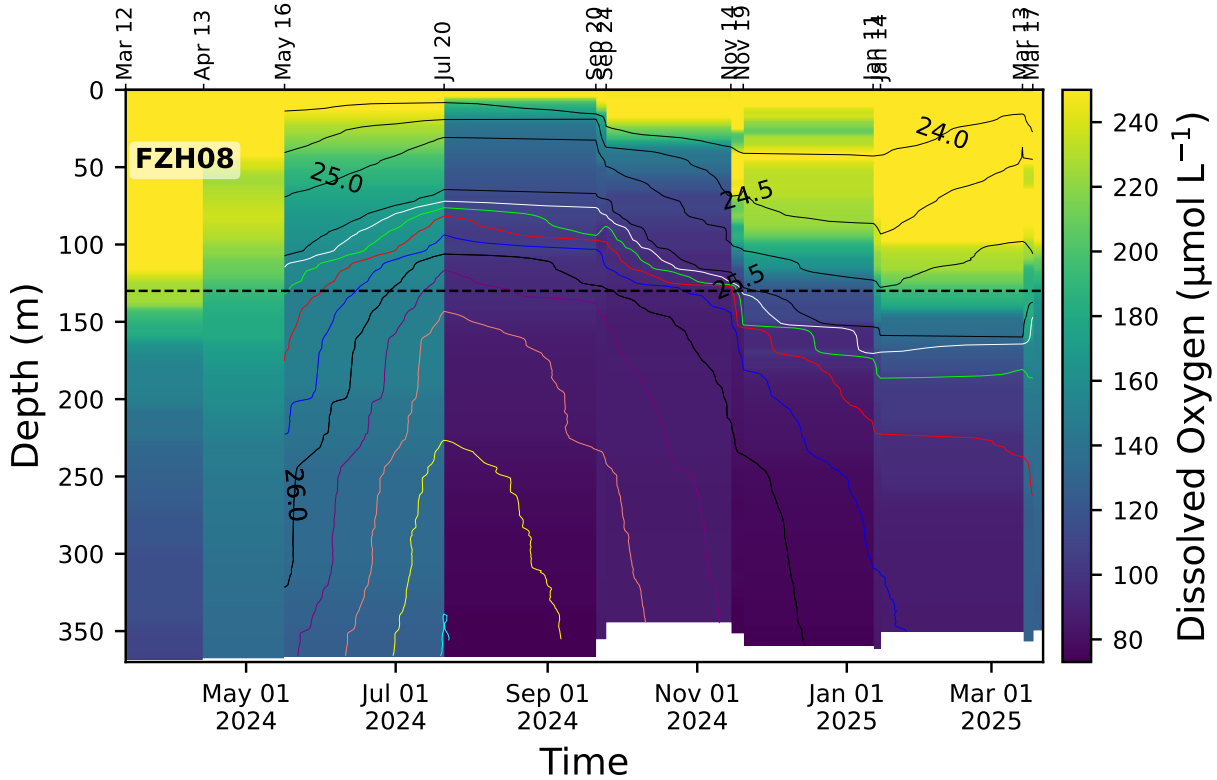


Figure 7: Oxygen ($\mu\text{mol L}^{-1}$) time series from March 2024 until August 2025. Contoured is potential density, σ_θ (kg m^{-3}): black isopycnals are spaced at $0.5 \sigma_\theta$, while the coloured lines represent isopycnals from $25.5 \sigma_\theta$ to $26.5 \sigma_\theta$ at intervals of 0.1 .

During the summer, renewal brings low oxygen conditions into the deep basin. During the summer, both on the shelf and in the basin (Figure 8), low oxygen conditions are associated with the upwelling of low oxygen water on the shelf, due to old pacific water already low

in O_2 being coupled with background respiration (Stevens et al., 2025b). When renewal occurs with this old, low O_2 water being the source water, basin properties adopt similar conditions to those on the shelf, and thus summer renewal brings low oxygen water to the basin. However, hypoxic conditions as seen on the shelf (Figure 8) are not observed in the FHS basin during renewal months. As has been previously suggested in previous years by (Evans, 2024), this dataset also suggests that mixing along the flow path modifies renewal water properties before the gravity current arrives in the deep basin, therefore oxygenating renewal water to some extent.

During the winter, renewal brings higher oxygen conditions into the deep basin, depending on adjacent shelf conditions, since vertical mixing and a deep mixed layer (Figure 3) brings higher oxygen conditions deeper in the water column (Figure 5). This oxygenates bottom water on the shelf, and under the right conditions, shelf bottom water is the source water for renewal (Figure 6). However, oxygen concentrations in the deep basin are not controlled by renewal source water alone. Mixing along the renewal flow path, including entrainment in a gravity current (Arneborg et al., 2004) and hydraulic jumps over the sill can further modify the oxygen content of inflowing water before it reaches the basin. In addition, background vertical mixing and possibly time varying respiration rates would continue to modify deep basin oxygen concentrations after renewal has occurred. As a result, the observed deep basin oxygen signal represents a superposition of source water properties, entrainment during renewal, vertical mixing, and biological oxygen consumption. Decoupling the relative importance of these processes therefore requires quantitative estimates of renewal and vertical mixing.

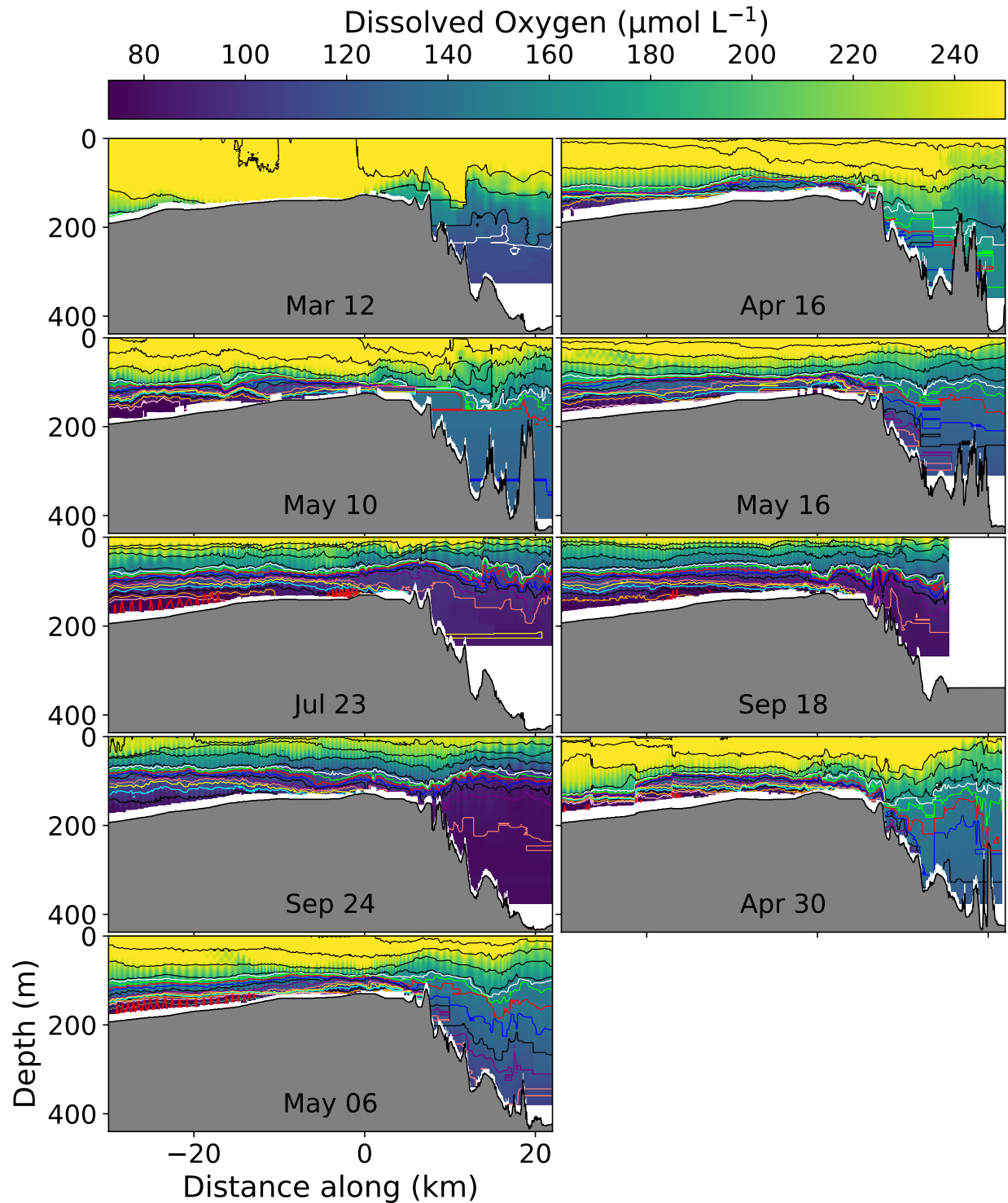


Figure 8: Oxygen [$\mu\text{mol L}^{-1}$] sections along the Calvert Line from March 2024 to May 2025. Panels are arranged in chronological order from left to right, top to bottom. Contours show potential density, σ_θ (kg m^{-3}): black isopycnals are spaced at $0.5 \sigma_\theta$, while the coloured lines highlight isopycnals from $25.5 \sigma_\theta$ to $26.5 \sigma_\theta$ at intervals of $0.1 \sigma_\theta$. Red contours near the ocean floor indicate hypoxic conditions or concentrations below $61 \mu\text{mol L}^{-1}$.

4 Discussion

Observations from repeated spring and summer transects suggest that deep water renewal in Fitz Hugh Sound (FHS) is not a single discrete event, but instead occurs frequently and may persist as a quasi continuous process throughout the renewal season, provided sufficiently dense shelf water is present at the Hakai Passage sill (Figures 3, 4, 9 and 10). It was also found that renewal of the FHS basin can occur in winter, while vertical mixing acts to smooth gradients between the surface and the basin. Along with the background respiration of organic matter, the superposition of all of these processes drive the observed annual oxygen signal (Figure 7). We can quantify the renewal process as well as the vertical mixing to begin to decouple the relative time varying importance of each of these processes.

4.1 Estimating a critical flow speed at the sill

Using a hydraulic control model, we can develop an upper bound estimate on the inflow rate of deep water through Hakai Passage (HP), assuming that the HP sill is the only place where renewal occurs (Figure 9). A renewal that is continuous would be similar to other fjords such as Trevor Channel and Alberni Inlet (Pawlowicz, 2017) and different from those that are discrete events such as Saanich Inlet (Soetaert et al., 2022).

The HP sill controls renewal, and this is justified since in April at the start of the 2024 renewal, density begins to increase at QCS07 (southern sill) at the same time density increases elsewhere but in much lesser amount than the HP sill (Figure 9). Throughout the renewal period, the water at QCS07 is much less dense than the HP sill, and so we conclude that the Hakai Passage sill must be the significant in terms of influencing renewal, and so we can use this sill for hydraulic control estimates.

To quantify the rate of exchange of the fjords basin water, we need to understand the baroclinic transport capacity of the mouth of the fjord. We can estimate this exchange with a two-layer hydraulic control model, under some assumptions (Arneborg et al., 2004).

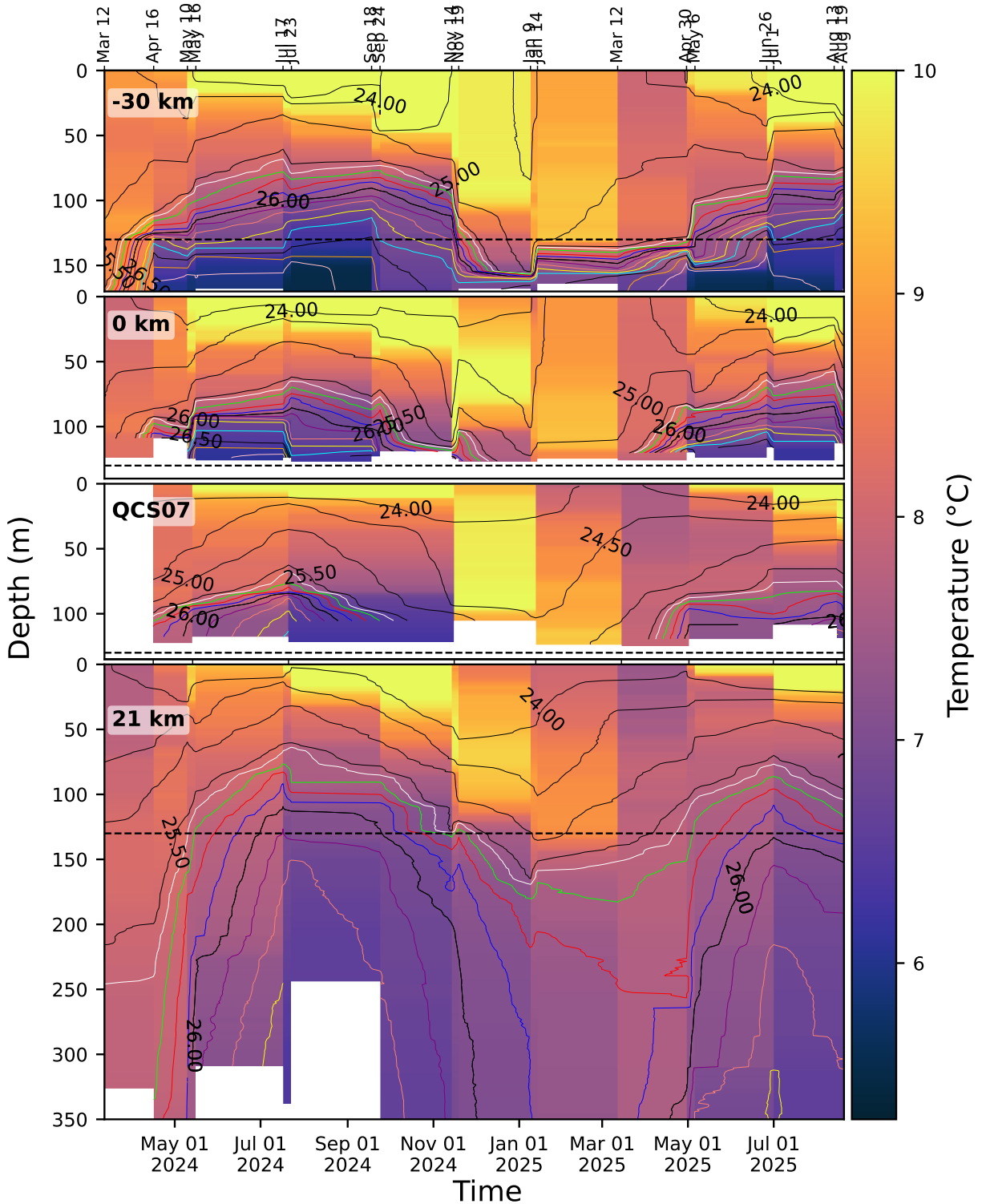


Figure 9: Potential temperature ($^{\circ}\text{C}$) time series from March 2024 until August 2025 at 4 locations. The dashed horizontal black line represents the HP sill depth (130 m). In order from top the bottom the panels are: the QCS shelf (-30 km), the HP sill (0 km), (near) the southern FHS sill (QCS07), and the FHS deep basin (21.1 km). Contoured is potential density, σ_θ (kg m^{-3}): black isopycnals are spaced at $0.5 \sigma_\theta$, while the coloured lines represent isopycnals from $25.5 \sigma_\theta$ to $26.5 \sigma_\theta$ at intervals of 0.1.

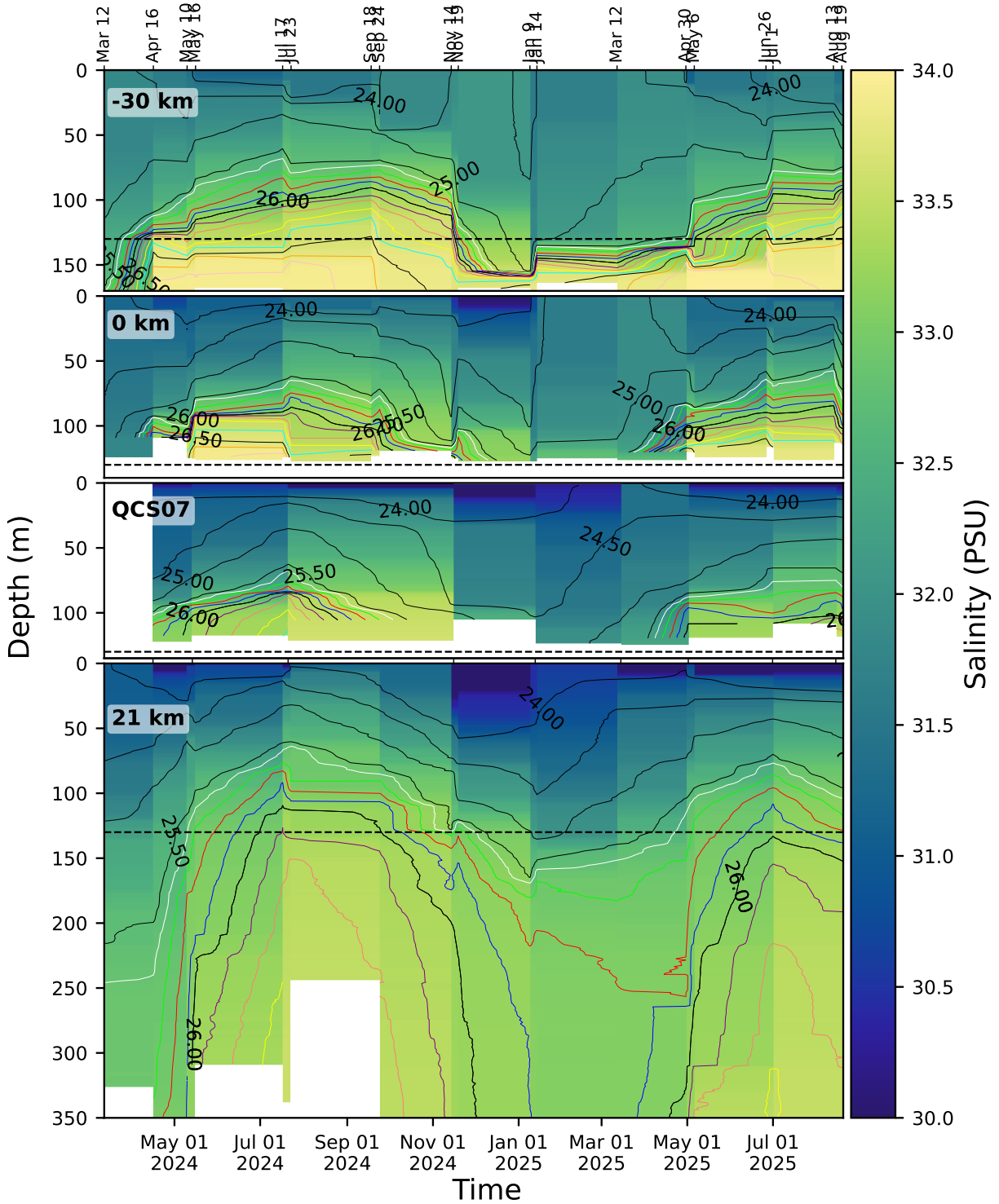


Figure 10: Salinity (PSU) time series from March 2024 until August 2025 at 4 locations. The dashed horizontal black line represents the HP sill depth (130 m). In order from top the bottom the panels are: the QCS shelf (-30 km), the HP sill (0 km), (near) the southern FHS sill (QCS07), and the FHS deep basin (21.1 km). Contoured is potential density, σ_θ (kg m^{-3}): black isopycnals are spaced at $0.5 \sigma_\theta$, while the coloured lines represent isopycnals from $25.5 \sigma_\theta$ to $26.5 \sigma_\theta$ at intervals of 0.1 .

We make the following assumptions:

1. If there is a hydraulic control, it is situated at the constriction that is the Hakai Passage sill, which is the easiest pathway for renewal water to enter FHS since it's the deepest and shortest flow path of the two sills, and where observations show the majority of dense renewal water is present during renewal months.
2. Barotropic currents are small relative to the baroclinic currents which implies flow should be continuous during the renewal and not influenced significantly by tides. We note that it is a well known phenomena that tides influence flow over a sill and thus we assume that this does not occur here for simplification, and thus the results here suggest an upper bound on inflow rates and residence times during renewal periods.
3. There are three distinct water layers present which allow for a two layer flow to occur with the top acting as a rigid lid. The deepest is a bottom inflow layer of dense water with isopycnals tilted down towards the deep basin overtop the sill. The second layer is an intermediate layer with isopycnals tilted opposite to the layer below it, indicating a return flow of basin water leaving the fjord. Finally, we assume the the surface layer to be frictionally balanced with the atmosphere above and the return flow layer below, therefore acting as a rigid lid, keeping the hydraulic control as a 2 layer flow. This is justified since the return flow isopycnal tilt of the middle layer seen in observations seems to diminish with proximity to the surface of ocean, indicating less and less return flow as it transitions towards a frictionally balanced surface layer.
4. If the above are true, then we have a two-layer flow, and the control section's inflow area can be approximated by a rectangular opening, whose inflow area height is approximated to be 30 m and width 2 km or area 60 000 m².

A simplified hydraulic control estimate under the above assumptions is generally thought of as a two-layer exchange, in which upwelling of dense water outside the fjord leads to a

two-layer hydraulic control with a deep inflow and a surface outflow. If we assume the sill is acting as a hydraulic control, limiting the flow rate over the sill, we can estimate the critical flow speed U using:

$$U \equiv \sqrt{g' h}$$

where g' is the reduced gravity, and h is the the lower flow layer thickness. g' is given by:

$$g' = g \frac{\rho_2 - \rho_1}{\rho_2}$$

where $g = 9.81 \text{ m s}^{-2}$ and ρ is the mean density of a given layer. We then estimate a renewal volumetric flux Q for each summer renewal transect that has a well defined renewal current into Hakai Passage. The results are shown in Table 1.

Table 1: Calculation results for a 2-layer hydraulic control over a sill. Columns show mean layer densities, reduced gravity (g'), lower-layer thickness (h), flow speed (U), and volumetric rate (Q).

Date	$\bar{\rho}_1$ (kg m ⁻³)	$\bar{\rho}_2$ (kg m ⁻³)	g' (m s ⁻²)	h (m)	U (m s ⁻¹)	Q (m ³ s ⁻¹)
2024-04-16	1024.54	1026.19	0.01581	30	0.69	41320
2024-05-10	1024.54	1026.06	0.01447	30	0.66	39530
2024-05-16	1024.79	1026.49	0.01626	30	0.70	41910
2024-07-17	1025.19	1026.62	0.01358	30	0.64	38300
2024-07-23	1025.10	1026.43	0.01276	30	0.62	37130
2025-04-30	1024.69	1026.29	0.01528	30	0.68	40620
2025-05-06	1024.71	1026.39	0.01611	30	0.70	41720
2025-06-26	1025.14	1026.47	0.01266	30	0.62	36980
2025-07-01	1024.95	1026.39	0.01378	30	0.64	38580
2025-08-13	1025.03	1026.27	0.01187	30	0.60	35800

These estimates reveal a volumetric flux of approximately $3.6\text{-}4.2 \times 10^4 \text{ m}^3 \text{ s}^{-1}$, and

renewal flow velocity of $0.6 - 0.7 \text{ m s}^{-1}$. Considering a basin volume of approximately $5.7 \times 10^{10} \text{ m}^3$ taken by integrating from the bottom topography up to 130 m depth for the entire deep basin, it would take between 15-19 days for a characteristic replacement of water below the sill depth. Considering the section plots in Figure 3, the first appearance of an isopycnal during a renewal and a consecutive lift of that isopycnal to the top of the deep basin on the next available transect, ie water of that density entering and filling the basin, tends to occur within a month (ie it has occurred by the time the next glider flies along) during the renewal months, with observed gravity currents in each transect (April, May, June, July). In some cases, multiple isopycnals lift within that time frame, indicating that renewal and complete flushing of the deep basin can occur in less than a month, consistent with our hydraulic control estimates. These estimates represent an upper bound on maximum renewal inflow rates under the assumptions made, and may be influenced by processes such as the tides or short term upwelling and downwelling fluctuations that we have not resolved here.

4.2 Mixing and oxygen modification during renewal

A continuous renewal regime as outlined above suggests a rapid adjustment of the basin to shelf properties, though we found that significant modification to renewal water occurs along the flow path. Dense water observed at the sill does not make it to the bottom of FHS in some transects without being modified, and hypoxic conditions seen on the shelf are not observed in the basin (Figures 3,4, and 8), indicating significant mixing is occurring. This mixing may occur over the sill or along the flow path due to entrainment, hydraulic jumps, and interactions with bathymetry.

We suggest that we can explain the mixing during renewal by considering what might happen to water as it mixes during a hydraulic jump at the sill, with less dense and higher O_2 water being entrained into the renewal gravity current. If we consider two water masses in density-oxygen space, one with lower density and higher oxygen and another with higher density but lower oxygen, conservative mixing would result in a water mass in between the

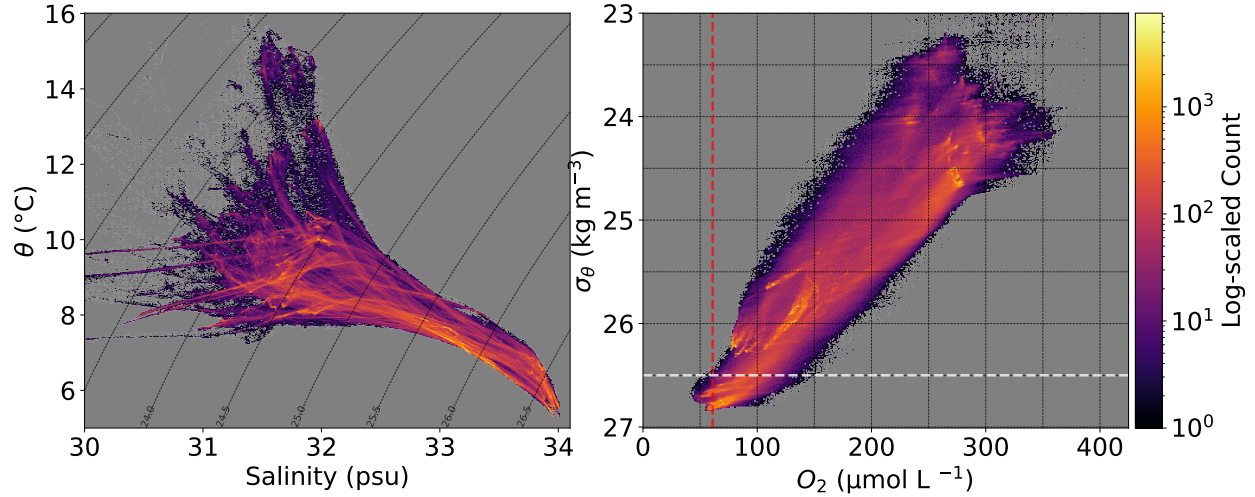


Figure 11: Histogram of all glider data from 2024 and 2025 for potential temperature θ ($^{\circ}\text{C}$) and salinity (psu) on the left panel, and potential density σ_{θ} (kg m^{-3}) plotted against oxygen $\mu\text{mol L}^{-1}$ on the right. The hypoxic limit of $61 \mu\text{mol L}^{-1}$ is plotted as a dashed red line. Data is binned to 0.01 ($^{\circ}\text{C}$), 0.01 psu, $0.01(\text{kg m}^{-3})$, and $1 \mu\text{mol L}^{-1}$. Density anomaly 26.5 kg m^{-3} is plotted as a dashed white line on the right panel.

two masses in parameter space (Figure 11). If the renewal water represented any end members on the high density low oxygen region in parameter space, then mixing has prevented hypoxic water from entering the basin, since water that exhibits hypoxia is almost always denser than the $26.5 \sigma_{\theta}$ isopycnal, and water of that density never makes it past the sill due to mixing with lighter water. The densest water at the sill is the $26.75 \sigma_{\theta}$ isopycnal while the densest water observed in FHS is the $26.4 \sigma_{\theta}$ isopycnal. This means that renewal water gets somewhat “oxygenated” over the sill or along the flow path as it mixes with higher oxygen water.

However, if hypoxia is becoming more widespread on the shelf, then in the case that water of lesser density was also to become hypoxic, mixing over the sill may not be sufficient to stop hypoxic water from flowing into the deep basin in FHS in the future. This highlights a need to quantify and decouple mixing, both laterally and vertically, from background respiration.

4.3 Vertical diffusion rate

We estimate vertical mixing and how it might modify oxygen concentrations over time by considering how much a conservative property is mixed out of the deep basin over time. We can model this using Fick's law of diffusion (with depth increasing downward):

$$F = -K \frac{\partial C}{\partial z}$$

where C is the concentration of the tracer, $\frac{\partial C}{\partial z}$ is the change in concentration of the tracer with depth, and K is a diffusion coefficient with units $\text{m}^2 \text{s}^{-1}$. The minus sign indicates that diffusion occurs down a gradient (from high concentration to low concentration). For example, if cold water is below warm water, heat diffuses downward, and if salty water is below less salty water, salt diffuses upwards.

If we consider an amount of some tracer that can change with depth and time $C(z, t)$ in a horizontal slab of depth z and area A , the amount of the tracer C at any given time or depth can be represented by:

$$\text{Amount of C} = A \cdot \Delta z \cdot C(z, t)$$

Then any change $\frac{d}{dt}(\text{Amount of C})$ will be given by any fluxes in or out of that slab. If the flux is happening in one direction, then the total change in that slab is:

$$\frac{d}{dt} (A \cdot \Delta z \cdot C(z, t)) = A \cdot F(z, t) - A \cdot F(z + \Delta z, t)$$

$$\frac{d}{dt} (\Delta z \cdot C(z, t)) = F(z, t) - F(z + \Delta z, t)$$

$$\Delta z \frac{\partial C}{\partial t} = F(z, t) - F(z + \Delta z, t)$$

$$\frac{\partial C}{\partial t} = \frac{F(z, t) - F(z + \Delta z, t)}{\Delta z}$$

$$\frac{\partial C}{\partial t} = -\frac{(F(z + \Delta z, t) - F(z, t))}{\Delta z}$$

in the limit as Δz goes towards zero, this is the definition of the derivative:

$$\frac{\partial C(z, t)}{\partial t} = -\frac{\partial F}{\partial z}$$

and since $F = -K \frac{\partial C}{\partial z}$ we can rewrite the above as:

$$\frac{\partial C}{\partial t} = \frac{\partial}{\partial z} \left(K \frac{\partial C}{\partial z} \right)$$

If we assume K is a constant, then we can pull it out of the derivative on the RHS:

$$\frac{\partial C}{\partial t} = K \frac{\partial^2 C}{\partial z^2}$$

which is the standard 1 dimensional diffusion equation. Now, if we want to solve this for the value of the constant K , we can integrate the equation vertically:

$$\int_{z_1}^{z_b} \frac{\partial C}{\partial t} dz = \int_{z_1}^{z_b} K \frac{\partial^2 C}{\partial z^2} dz$$

rewriting as:

$$\frac{\partial}{\partial t} \int_{z_1}^{z_b} C dz = K \int_{z_1}^{z_b} \frac{\partial^2 C}{\partial z^2} dz$$

Which means that the change in the total tracer in the basin depends only on the gradients at the boundaries. This is useful because we can evaluate this and apply our no flux condition at the bottom of the basin $F(z_b) = 0$:

$$\frac{\partial}{\partial t} \int_{z_1}^{z_b} C dz = K \int_{z_1}^{z_b} \frac{\partial^2 C}{\partial z^2} dz = K \left[\frac{\partial C}{\partial z} \right]_{z_1}^{z_b} = K \left(\frac{\partial C}{\partial z} \Big|_{z_b} - \frac{\partial C}{\partial z} \Big|_{z_1} \right)$$

Evaluating at the bottom boundary:

$$F(z_b) = -K \frac{\partial C}{\partial z} \Big|_{z_b} = 0 \quad \Rightarrow \quad \frac{\partial C}{\partial z} \Big|_{z_b} = 0$$

so

$$\frac{\partial}{\partial t} \int_{z_1}^{z_b} C dz = -K \frac{\partial C}{\partial z} \Big|_{z_1}$$

Next let's define the mean concentration of the tracer C with depth in the basin as:

$$\bar{C} = \frac{1}{H} \int_{z_1}^{z_b} C dz, \quad H = z_b - z_1$$

and so the diffusion equation becomes:

$$H \frac{\partial \bar{C}}{\partial t} = -K \frac{\partial C}{\partial z} \Big|_{z_1}$$

or finally:

$$K = -H \frac{\partial \bar{C} / \partial t}{\frac{\partial C}{\partial z} \Big|_{z_1}}$$

which is valid under the assumptions that:

- K is an average at z_1 assuming $\frac{\partial C}{\partial z}$ is the same everywhere on that isopycnal
- There is no diffusive flux at the bottom
- The deep basin behaves like a well mixed control volume below z_1
- The flux through the interface can be represented by the gradient at z_1 , which we will take to be the average gradient between 130 m and 150 m depth, which is the ap-

proximate location of the deepest parts of the thermocline/halocline/pycnocline before properties change much more weakly with depth, as seen from the earlier plots. This means that now we have a way to estimate a value of K numerically if we take $\frac{\partial \bar{C}}{\partial t} \approx \frac{\Delta C}{\Delta t}$ where ΔC and Δt are just the change in a value between consecutive transects.

Solving for K for temperature, salinity, and density for both glider data at 21.1 km along as well as the Hakai CTD data from FHZ08 yields the results as seen in Table 2 for all winter transects. Estimates reveal vertical diffusivity values of magnitude $0.9\text{-}3.9 \times 10^{-3} (\text{m}^2 \text{s}^{-1})$, other than some anomalously low K_z values from the glider between the January 9 and January 14 transects on the order of $10^{-5} (\text{m}^2 \text{s}^{-1})$. These values are similar to those of other regions in B.C. For example, K_z for the Strait of Georgia has been estimated to be on the order of $1.1 \times 10^{-3} \text{ m}^2 \text{ s}^{-1}$ (Masson, 2002), and for Indian Arm $K_z \approx 0.5 - 15 \times 10^{-3} \text{ m}^2 \text{ s}^{-1}$ (de Young and Pond, 1988).

Table 2: Estimated vertical diffusivity K_z ($\text{m}^2 \text{s}^{-1}$) between consecutive profiles using a vertically integrated budget method evaluated at the top of the deep basin. Estimates are shown for density, potential temperature, and salinity using both glider and Hakai observations.

Source	Start Date	End Date	$K_{z,\rho}$	$K_{z,T}$	$K_{z,S}$
Hakai	2024-09-20	2024-09-24	3.51×10^{-3}	3.88×10^{-3}	3.42×10^{-3}
Hakai	2024-09-24	2024-11-14	2.69×10^{-3}	2.92×10^{-3}	2.66×10^{-3}
Glider	2024-09-25	2024-11-14	1.62×10^{-3}	1.55×10^{-3}	1.67×10^{-3}
Glider	2024-11-14	2024-11-19	1.62×10^{-3}	1.74×10^{-3}	1.63×10^{-3}
Hakai	2024-11-14	2024-11-19	3.60×10^{-3}	2.97×10^{-3}	3.90×10^{-3}
Glider	2024-11-19	2025-01-09	1.12×10^{-3}	1.33×10^{-3}	1.08×10^{-3}
Hakai	2024-11-19	2025-01-11	1.17×10^{-3}	1.25×10^{-3}	1.16×10^{-3}
Glider	2025-01-09	2025-01-14	2.50×10^{-5}	5.57×10^{-5}	2.18×10^{-5}
Hakai	2025-01-11	2025-01-14	1.07×10^{-3}	9.29×10^{-4}	1.10×10^{-3}

5 Conclusions

This study used high resolution glider transects and supporting Hakai CTD survey data to examine deep water renewal in Fitz Hugh Sound between March 2024 and August 2025. The results suggest that renewal is not limited to a single discrete event but instead can occur frequently or even continuously during spring and summer, with winter deep water renewal occurring on occasion, provided that cold, dense water is present on the Queen Charlotte Sound shelf near the sill. Basin water temperature and salinity properties adjust rapidly to those of the incoming renewal water, with flushing of the deep basin occurring within weeks of observed ideal renewal conditions at the sill. This is consistent with at least one other fjord system on the BC coast with a deep sill (Pawlowicz, 2017). Significant mixing occurs over the sill region during a renewal, possibly due to hydraulic jumps and turbulent mixing, reducing the density and modifying the oxygen characteristics of renewal water.

Although dense source waters on the QCS shelf were occasionally hypoxic, hypoxia was not observed in the Fitz Hugh Sound deep basin during the study period, since the density of water previously associated with hypoxia (Stevens et al., 2025a) wasn't observed in the FHS basin during our study period. Since water as dense as $26.75 \sigma_\theta$ was observed over the sill, but that water never made it into the deep basin, we suggest that mixing over the Hakai Passage sill and along the flow path entrains less dense, and higher oxygen water, raising oxygen concentrations above hypoxic thresholds before the water reaches the basin, as was previously suggested by (Evans, 2024). Hydraulic jumps and turbulent mixing are likely the key mechanisms modifying renewal water properties during the renewal. Oxygen in the basin consistently decreased through the summer and increased in the winter, pointing to an interplay of renewal, mixing, and background respiration.

Simple two-layer hydraulic control estimates yielded upper bound renewal velocities of $0.6\text{--}0.7 \text{ m s}^{-1}$ and volumetric fluxes of $3.6\text{--}4.2 \times 10^4 \text{ m}^3 \text{ s}^{-1}$, consistent with observed isopycnal lift and replacement times of less than one month, however these calculations assume no mixing. Since mixing was observed at the sill and along the flow path, these replacement time

estimates represent an upper bound on the basin flushing rate during a renewal. This work establishes a framework for considering renewal timescales in this type of deep silled fjord and the role of renewal in basin ventilation, especially during winter when the occurrence of renewal is less apparent and perhaps weaker than during the summer. Higher temporal resolution would be required to understand winter renewal in greater detail than is discussed in this thesis.

Vertical diffusivity estimates yielded values in the range of $0.9\text{-}3.9 \times 10^{-3}(\text{m}^2 \text{ s}^{-1})$. These values are similar to those in other regions in B.C. such as the Strait of Georgia ($1.1 \times 10^{-3} \text{ m}^2 \text{ s}^{-1}$, (Masson, 2002)), and Indian Arm ($K_z \approx 0.5 - 15 \times 10^{-3} \text{ m}^2 \text{ s}^{-1}$, (de Young and Pond, 1988)), suggesting this basin is similar energetically as compared to other regions.

Future work might further develop a better understanding of the energetics of the basin using the glider data and ongoing data collection in the region. Other analyses might include oxygen conservation budgeting to decouple respiration from vertical mixing, which could use the K_z estimates from this work. There also exists a time series of CTD measurements in Hakai Passage at the sill from a mooring program from the Institute of Ocean Sciences collected between 2017 and 2023 (Stevens et al., 2025b), and an analysis of this time series may give insight into whether our hydraulic control estimates are well justified or not (by determining if renewal is occurring continuously or not). For this analysis, comparisons during renewal would have to be made with data from gliders or Hakai in FHS at a similar time. Another analysis of a time series of deep basin dives at roughly 21 km along the transect in March 2026 might help understanding the effect of the tidal cycle and other short term fluctuations in the deep basin. Finally, if a model were to be built and used in this region, comparisons could be made to the general circulation framework established in this study for model validation.

The framework of the physical processes described in this work are generally consistent with work done for other fjord systems in BC, though winter renewal is more rarely mentioned in the literature. This work has implications for understanding biogeochemical cycles in the

region and may be useful for assessing whether projected increases in shelf hypoxia could eventually overcome the buffering effect of sill mixing for Fitz Hugh Sound. Such efforts are essential for understanding the long term vulnerability of Fitz Hugh Sound and connected inlets to decreasing oxygen concentrations and hypoxia on the shelf under a changing climate.

6 Supplementary remarks

I initially began this honours thesis work with C-PROOF in May 2025 under a summer SURA funding award, and during that time, I had the opportunity to be trained in and then be responsible for glider recovery, turnaround, and deployment for the SeaExplorer glider, dfo-eva035. This supported the C-PROOF glider team in maintaining a time series of transects being collected on the Southern Vancouver Island shelf starting in Barkley Sound. This role involved driving to Bamfield every three weeks for a portion of the summer, taking a boat ride to Barkley Sound to recover the glider with support from the BMSC foreshore staff, and then working through the turnaround procedure. The turnaround procedure involves a 1.5 day process of performing physical checks on the glider, putting it through two charge cycles, transferring and uploading data to the C-PROOF server and creating backups, and then testing all of the main functions of a glider by piloting it through "simulation dives" while on land. Once all of the checks had been completed, and the glider was charged, I would redeploy the glider, again with boat support from the BMSC staff, while coordinating with an onshore glider pilot who would communicate with the glider via satellite. Once the glider was in the water, and we could be sure the glider could dive and surface autonomously (such that it wouldn't sink to the bottom of the ocean never to be seen again), we could detach it from a rope and buoy, and the pilot would send the glider off on its next mission.

Some of the other opportunities that arose from this experience, while working a few days at a time in Bamfield, included socializing and networking with unique and inspiring people. I met many of the summer students taking courses at BMSC, and met and had conversations

with Stickleback researchers from around the world (when a glider turnaround coincided with a triennial international Stickleback conference). It was also a privilege to receive further technical training to develop my skills in operating oceanographic field equipment (gliders) outside of the sampling techniques and procedures learned through UVic's oceanography courses.

Furthermore, the combination of summer SURA research and honours research position allowed me to spend a significant amount of time reading and learning about physical oceanography in BC both historically and up to the present. I was also invited to attend the UVic Ocean Science Journal Club, where researchers and graduate students meet for an hour every few weeks to discuss a recent paper in the field. This has allowed me practice in reading, understanding, and critiquing scientific papers, as well as expanding my knowledge of oceanography, which are valuable skills in science and for my career.

7 Acknowledgements

I would like to sincerely thank my supervisor, Dr. Jody Klymak, for his ongoing support and mentorship to help me become a better scientist, and for providing me with an ongoing opportunity to dive into the world of ocean physics. I would like to thank Dr. Tetjana Ross, Dr. Wiley Evans, Dr. Giuliana Berden, Lauryn Talbot, Polina Erofeeva, Wyatt Cottriel, Ian Baker, Jamie Daniel, and Becky Brooks for their input, conversations, and insight helping me to improve the quality of this work. I would like to thank Nick Harper and James Pegg for glider turnaround training and for all of their efforts in maintaining the C-PROOF glider fleet, along with the staff at the Hakai Institute for their continued Calvert Line glider support. I would like to thank the staff and students at BMSC for the support during fieldwork, the amazing meals at the cafeteria, and evenings spent socializing in the summer of 2025. Finally, I would like to thank Fred Gibson, also known as the music producer Fred Again..., for providing the world with a vast library of music, along with countless live

and ambient sets that I listened to for hundreds of hours (as reported by my Spotify and SoundCloud listening statistics) during the year on which I worked on this thesis.

References

- Lars Arneborg, Carina Erlandsson, Bengt Liljebladh, and Anders Stigebrandt. The rate of inflow and mixing during deep-water renewal in a sill fjord. *Limnology and Oceanography*, 49:768–777, 05 2004. doi:[10.4319/lo.2004.49.3.0768](https://doi.org/10.4319/lo.2004.49.3.0768).
- Brad de Young and Stephen Pond. The deepwater exchange cycle in indian arm, british columbia. *Estuarine, Coastal and Shelf Science*, 26(3):285–308, 1988.
- A.J. Dodimead and R.H. Herlinveaux. Some oceanographic features of the waters of the Central British Columbia Coast. Technical Report 70, Fisheries Research Board of Canada, Biological Station, Nanaimo, B.C., July 1968. URL <https://waves-vagues.dfo-mpo.gc.ca/Library/32947.pdf>. Pacific Oceanographic Group.
- Wiley Evans. Biogeochemical observations on the B.C. margin during 2023. In J. L. Boldt, E. Joyce, S. Tucker, S. Gauthier, and H. Dosser, editors, *State of the Physical, Biological and Selected Fishery Resources of Pacific Canadian Marine Ecosystems in 2023*, volume 3598, chapter 18, pages viii + 315. Canadian Technical Report of Fisheries and Aquatic Sciences, Nanaimo, BC, 2024.
- David M. Farmer and Howard J. Freeland. The physical oceanography of fjords. *Progress in Oceanography*, 12:147–220, 1983. doi:[10.1016/0079-6611\(83\)90004-6](https://doi.org/10.1016/0079-6611(83)90004-6).
- Jody Klymak and Tetjana Ross. C-PROOF underwater glider deployment datasets. Dataset, 2025. URL <https://doi.org/10.82534/44DS-K310>.
- C. C. Manning, R. C. Hamme, and A. Bourbonnais. Impact of deep-water renewal events on fixed nitrogen loss from seasonally anoxic Saanich Inlet. *Marine Chemistry*, 122(1-4):1–10, 2010. doi:[10.1016/j.marchem.2010.08.002](https://doi.org/10.1016/j.marchem.2010.08.002). URL <https://doi.org/10.1016/j.marchem.2010.08.002>.

-
- D. Masson. Deep water renewal in the strait of georgia. *Estuarine, Coastal and Shelf Science*, 54(1):115–126, 2002. doi:[10.1006/ecss.2001.0833](https://doi.org/10.1006/ecss.2001.0833).
- R. Pawlowicz. Seasonal cycles, hypoxia, and renewal in a coastal fjord (Barkley Sound, British Columbia). *Atmosphere-Ocean*, 55(4-5):264–283, 2017. doi:[10.1080/07055900.2017.1374240](https://doi.org/10.1080/07055900.2017.1374240). URL <https://doi.org/10.1080/07055900.2017.1374240>.
- G. L. Pickard. Oceanographic features of inlets in the British Columbia Mainland Coast. *Journal of the Fisheries Research Board of Canada*, 18(6):907–999, 1961. Received for publication May 15, 1961.
- G. Soetaert, R. C. Hamme, and E. Raftery. Renewal of seasonally anoxic Saanich Inlet is temporally and spatially dynamic. *Frontiers in Marine Science*, 9:1001146, 2022. doi:[10.3389/fmars.2022.1001146](https://doi.org/10.3389/fmars.2022.1001146). URL <https://doi.org/10.3389/fmars.2022.1001146>.
- S. W. Stevens, C. Hannah, W. Evans, J. Klymak, T. Ross, and S. Waterman. Drivers of oxygen variability on the Canadian Pacific Shelf in the context of emerging hypoxia. *ESS Open Archive*, March 2025a. doi:[10.22541/essoar.174117442.29335954/v1](https://doi.org/10.22541/essoar.174117442.29335954/v1). URL <https://doi.org/10.22541/essoar.174117442.29335954/v1>. Preprint.
- Samuel Stevens, Charles Hannah, W. Evans, Jody Klymak, S. Waterman, and Tetjana Ross. Dissolved oxygen variability on the canadian pacific shelf: Trends, drivers, and projections in the context of emerging hypoxia in queen charlotte sound. *Global Biogeochemical Cycles*, 39, 08 2025b. doi:[10.1029/2025GB008608](https://doi.org/10.1029/2025GB008608).

Appendix

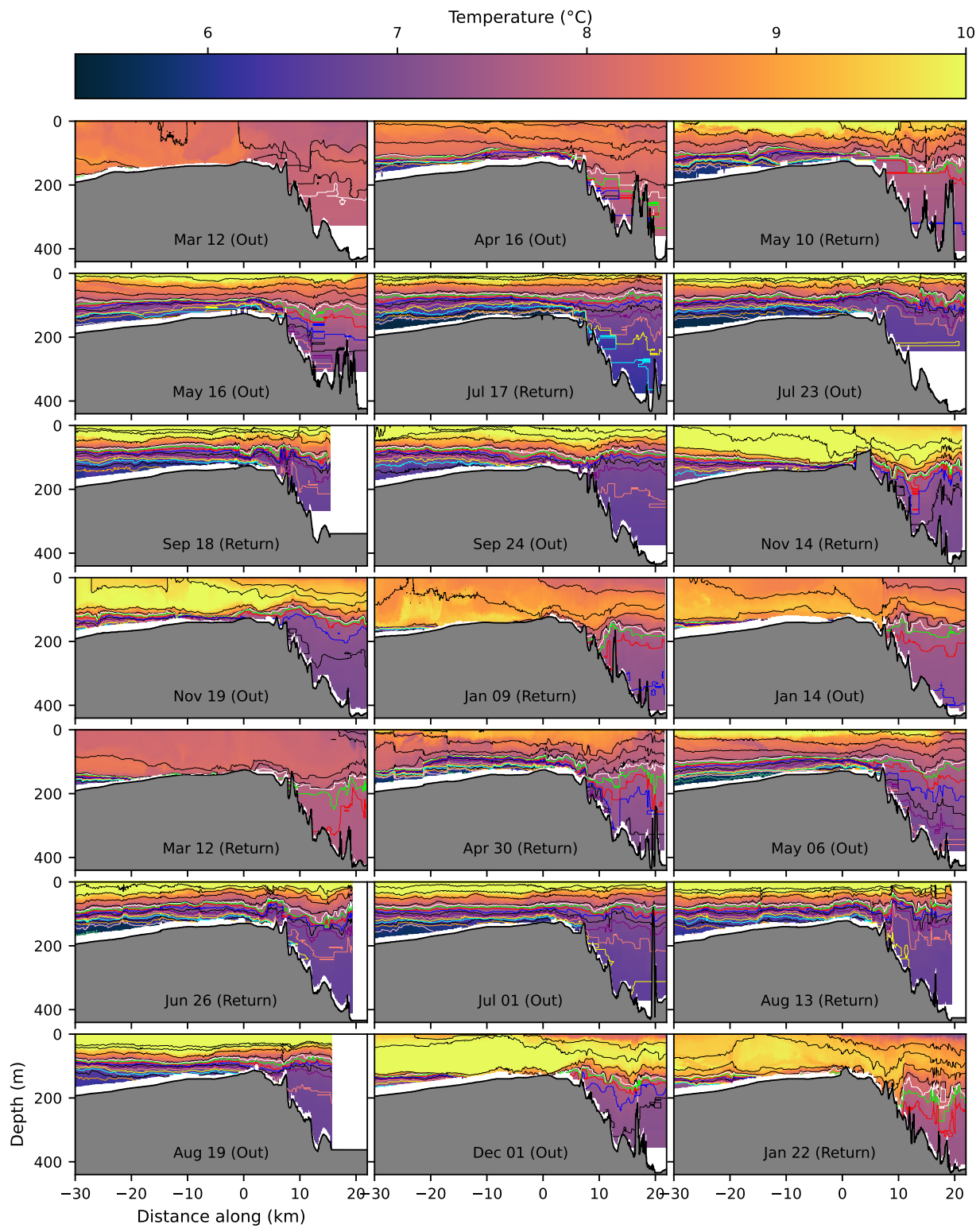


Figure 12: Potential temperature θ ($^{\circ}\text{C}$) sections along the Calvert Line from March 2024 to January 2026. Panels are arranged in chronological order from left to right, top to bottom. Contours show potential density, σ_{θ} (kg m^{-3}): black isopycnals are spaced at $0.5 \sigma_{\theta}$, while the coloured lines highlight isopycnals from $25.5 \sigma_{\theta}$ to $26.5 \sigma_{\theta}$ at intervals of $0.1 \sigma_{\theta}$.

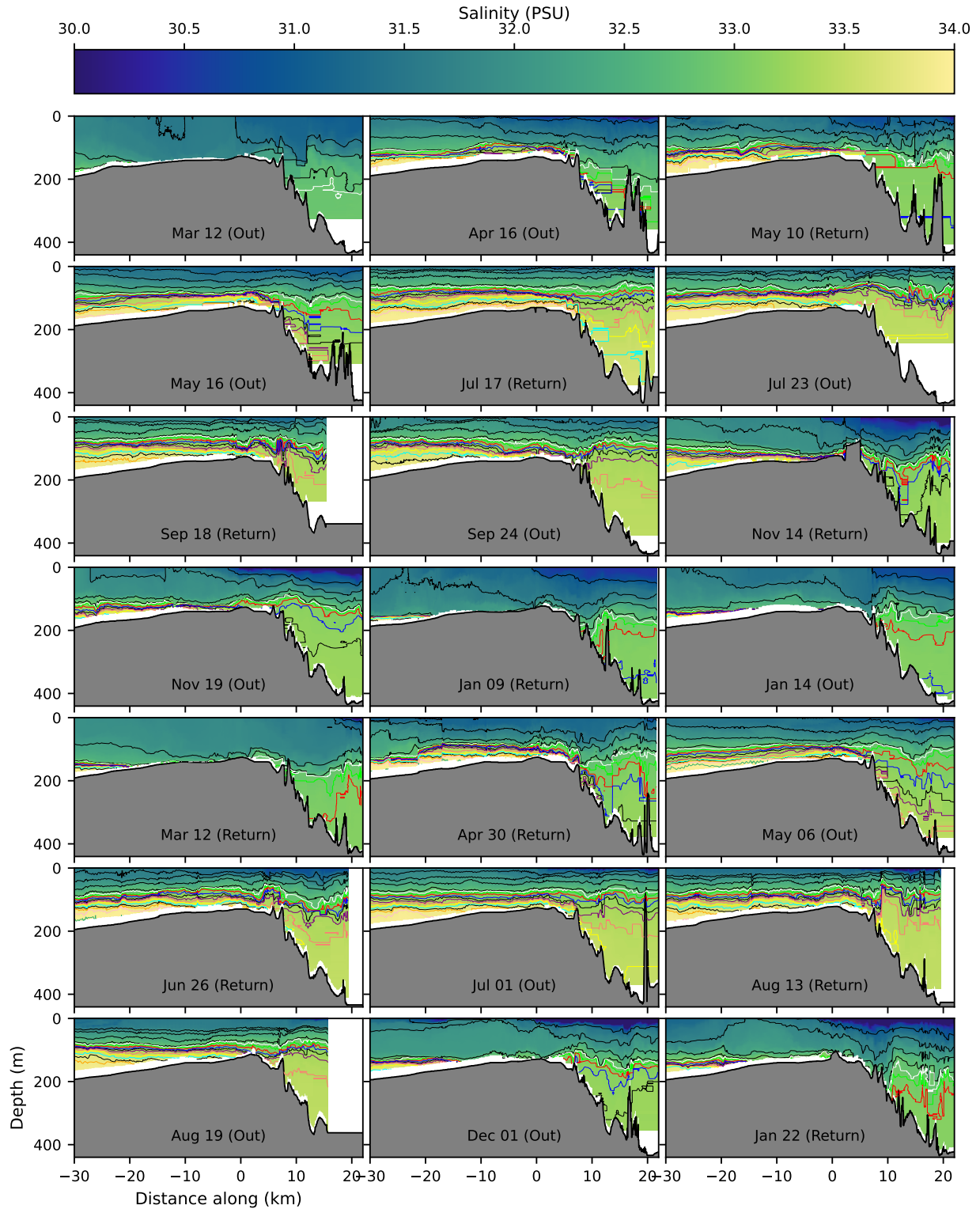


Figure 13: Salinity (PSU) sections along the Calvert Line from March 2024 to January 2026. Panels are arranged in chronological order from left to right, top to bottom. Contours show potential density, σ_θ (kg m^{-3}): black isopycnals are spaced at $0.5 \sigma_\theta$, while the coloured lines highlight isopycnals from $25.5 \sigma_\theta$ to $26.5 \sigma_\theta$ at intervals of $0.1 \sigma_\theta$.